JACS
JOURNAL OF THE AMERICAN CHEMICAL SOCIETY

Communication

pubs.acs.org/JACS

The B_{35} Cluster with a Double-Hexagonal Vacancy: A New and More Flexible Structural Motif for Borophene

Wei-Li Li,[†] Qiang Chen,[‡] Wen-Juan Tian,[‡] Hui Bai,[‡] Ya-Fan Zhao,[§] Han-Shi Hu,[§] Jun Li,*[,§] Hua-Jin Zhai,*[,‡] Si-Dian Li,*[,‡] and Lai-Sheng Wang*[,†]

[†]Department of Chemistry, Brown University, Providence, Rhode Island 02912, United States

[‡]Nanocluster Laboratory, Institute of Molecular Science, Shanxi University, Taiyuan 030006, China

[§]Department of Chemistry & Key Laboratory of Organic Optoelectronics and Molecular Engineering of Ministry of Education, Tsinghua University, Beijing 100084, China

Supporting Information

ABSTRACT: Elemental boron is electron-deficient and cannot form graphene-like structures. Instead, triangular boron lattices with hexagonal vacancies have been predicted to be stable. A recent experimental and computational study showed that the B_{36} cluster has a planar C_{6v} structure with a central hexagonal hole, providing the first experimental evidence for the viability of atom-thin boron sheets with hexagonal vacancies, dubbed borophene. Here we report a boron cluster with a double-hexagonal vacancy as a new and more flexible structural motif for borophene. Photoelectron spectrum of B_{35}^- displays a simple pattern with certain similarity to that of B_{36}^-. Global minimum searches find that both B_{35}^- and B_{35} possess planar hexagonal structures, similar to that of B_{36}, except a missing interior B atom that creates a double-hexagonal vacancy. The closed-shell B_{35}^- is found to exhibit triple π aromaticity with 11 delocalized π bonds, analogous to benzo(g,h,i)perylene ($C_{22}H_{12}$). The B_{35} cluster can be used to build atom-thin boron sheets with various hexagonal hole densities, providing further experimental evidence for the viability of borophene.

Two-dimensional (2D) atom-thin boron sheets have attracted increasing attention. Early theoretical investigations showed that graphene-like boron sheets with a honeycomb lattice are unstable; instead, boron tends to form buckled all-triangular lattices.[1−4] More recent theoretical studies predicted a new type of planar boron sheets, consisting of triangular lattices with hexagonal vacancies, to be more stable and suitable to form boron nanotubes.[5,6] The role of the hexagonal hole has been rationalized in term of chemical bonding.[7] Various forms of monolayer boron structures have been considered with different vacancy densities and arrangements.[8−13] However, it was not clear if such extended 2D boron nanostructures can be realized experimentally, even though possible methods have been proposed theoretically.[14,15]

Over the past decade, combined experimental and theoretical studies have allowed the structures and chemical bonding of small boron clusters to be systematically elucidated.[16−24] The structural, electronic, and chemical bonding properties of size-selected boron clusters are fascinating and help lay the foundation for the rational design of new boron nanostructures. In contrast to bulk boron, which consists of various 3D cage motifs, small boron clusters have been found to be planar or quasi-planar. Negatively charged boron clusters (B_n^-) have been characterized systematically via joint photoelectron spectroscopy (PES) and quantum chemistry calculations to be planar at least up to $n = 25$.[16−23] Cationic boron clusters (B_n^+) have been shown to be planar up to $n = 16$ on the basis of ion mobility experiment.[24] Neutral boron clusters are more challenging experimentally. An UV-IR double-resonance experiment did not detect the double-ring B_{20},[25] which was suggested to be the first 3D neutral boron cluster.[18] Chemical bonding in the 2D boron clusters is dominated by σ and π delocalization, giving rise to the concepts of aromaticity, antiaromaticity, and multiple aromaticity.[16−23,26−28] Some boron clusters have been shown to have intriguing fluxional behaviors that have inspired the proposal of molecular Wankel motors.[29−31]

A major breakthrough in the investigation of boron clusters has occurred recently, where B_{36}^- and B_{36} have been discovered to possess 2D structures with a central hexagonal hole.[32] The B_{36} cluster can be viewed as the embryo for the formation of extended 2D boron sheets with hexagonal vacancies, providing the first experimental evidence for the potential viability of such boron nanostructures. A name, borophene, was coined to designate the putative atom-thin boron sheets, in analogy to graphene.[32] The hexagonal vacancy seems to be the defining structural feature of medium-sized boron clusters above $n = 30$. A subsequent investigation found that B_{30}^- is chiral, possessing a pair of quasiplanar enantiomers with a hexagonal hole.[33] Most recently, it has been found that the B_{40}^- cluster consists of two nearly degenerate structures, a planar structure featuring two adjacent hexagonal holes and a 3D cage structure, the first all-boron fullerene, dubbed borospherene.[34]

Here we report a PES and theoretical study on the B_{35}^- and B_{35} clusters, which are found to be the smallest planar boron clusters containing a double-hexagonal vacancy (DHV) with two adjacent hexagonal holes. This structure is similar to the hexagonal B_{36} cluster with a missing interior B atom. Chemical bonding analyses reveal a triple π aromatic system for the closed-shell B_{35}^-, analogous to the benzo(g,h,i)perylene ($C_{22}H_{12}$)

Received: July 22, 2014
Published: August 20, 2014

molecule. Most significantly, the B_{35} cluster can be viewed as a new and more flexible motif to construct various types of borophene, containing DHVs or mixed hexagonal holes and DHVs.

The photoelectron spectrum of B_{35}^- at 193 nm is shown in Figure 1 (see the Supporting Information for experimental details). The low binding energy band X, which represents the electron detachment transition from the ground state of B_{35}^- to that of neutral B_{35}, occurs at a vertical detachment energy (VDE) of 4.06 ± 0.05 eV. Since no vibrational structures are resolved for band X, the adiabatic detachment energy (ADE) is evaluated by drawing a straight line along the leading edge and then adding the instrumental resolution to the intersection with the binding energy axis. The ADE thus evaluated is 3.96 ± 0.05 eV, which also represents the electron affinity of neutral B_{35}. Band A appears at ~5.0 eV, which is separated from band X by an energy gap of ~0.9 eV as evaluated from the VDE difference of the two bands. Band B is prominent and broad, centering at 5.35 ± 0.05 eV and hinting it may contain multiple detachment transitions. A well-separated band C is observed at 5.93 ± 0.05 eV. The overall spectral pattern is well-structured and relatively simple, providing a definitive electronic fingerprint for B_{35}^- and the corresponding neutral B_{35}. It is interesting to note that the spectrum of B_{35}^- is somewhat similar to that of B_{36}^-,[32] except the latter contains an extra low binding energy feature at a VDE of 3.3 eV. This observation suggests that the structure of B_{35}^- may be related to the hexagonal B_{36}^-.

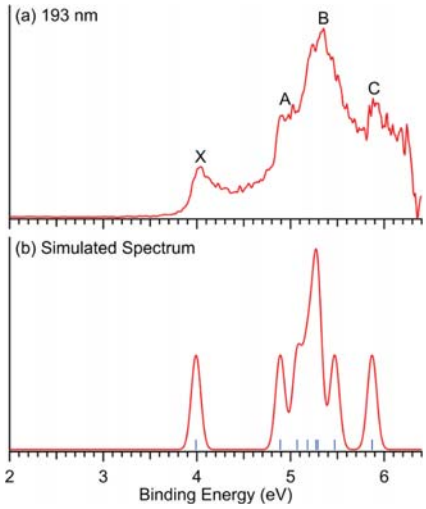

Figure 1. Experimental photoelectron spectrum of B_{35}^- at 193 nm (a), compared to the simulated spectrum at the PBE0 level (b). The simulation was done for the global-minimum C_s (^{1}A′) structure by fitting the calculated VDEs with unit-area Gaussian functions of 0.05 eV half-width. The vertical lines in (b) represent the calculated VDEs.

Global minimum searches were accomplished using the minima hopping algorithm[35] and a guided basin-hopping program called TGmin,[32] in combination with manual structural constructions, as described in the Supporting Information (SI). The global minimum of B_{35}^- (C_s, ^{1}A′) is shown in Figure 2, along with its corresponding neutral structure (C_s, ^{2}A″). These structures are quasi-planar with an overall hexagonal shape, in which the B atoms are triangular close-packed except for the two adjacent hexagonal holes. Alternative optimized anion and neutral structures within 1.5 eV are given in Figures S1 and S2, respectively, in the SI. The nearest competing structures are 0.52 and 0.27 eV higher in energy for the anion and neutral, respectively, suggesting that the B_{35}^- (C_s, ^{1}A′) and B_{35} (C_s, ^{2}A″) structures with the DHV are quite stable species. The relative energies at the CCSD(T) level are 0.56 and 0.38 eV for the anion and neutral, respectively, further confirming the stability of the C_s B_{35}^- (^{1}A′) and C_s B_{35} (^{2}A″) (see SI). The lowest-energy 3D structures are cage-like, being 0.85 and 0.72 eV above the global minima, respectively, for the anion and neutral.

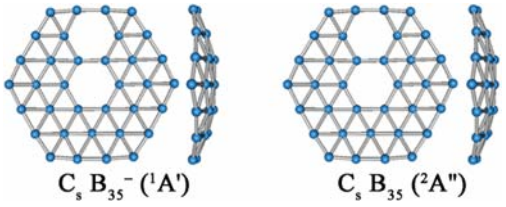

Figure 2. Optimized global-minimum structures of B_{35}^- (C_s, ^{1}A′) and neutral B_{35} (C_s, ^{2}A″) at the PBE0/6-311+G* level.

To confirm that the C_s (^{1}A′) structure is the true global minimum for B_{35}^-, we calculated its VDEs, using the time-dependent DFT method with the PBE0 functional (TD-PBE0),[36] to compare with the experimental data. The ADE was calculated via the total energy difference (i.e., ΔSCF method), whereas the VDEs for the anionic clusters were calculated using the combined ΔSCF-TDDFT approach.[37,38] PBE0 has been proved to be reliable in boron clusters in this size range.[23,32−34] As shown in Table S1 in the SI, the calculated ground-state VDE is 3.99 eV, in excellent agreement with the experimental value of 4.06 eV. The ground-state ADE is calculated to be 3.91 eV, compared with the experimental value of 3.96 eV. The calculated VDE for the second detachment channel (4.89 eV) is in good agreement with band A at ~5.0 eV. The computed VDEs for the next five detachment channels are closely spaced ranging from 5.07 to 5.47 eV, which should correspond to the broad and prominent band B covering the same energy range. Following a small energy gap, the next calculated detachment transition is at 5.87 eV, in good agreement with band C at 5.93 eV. The simulated spectrum (Figure 1b), obtained by fitting the calculated VDEs with unit-area Gaussians, is almost in quantitative agreement with the experimental spectrum, lending considerable credence to the identified global minimum of the quasiplanar hexagonal B_{35}^- with the DHV.

The structure of neutral B_{35} is similar to the anion with little geometry change (see Figure S4 for detailed structural parameters). The overall structures of B_{35}^- and B_{35} resemble closely the structures of the hexagonal B_{36}^- and B_{36}, respectively, except the additional hexagonal hole in the former. Both B_{36}^- and B_{36} possess hexagonal structures with a central hexagonal hole. They can also be viewed as consisting of three concentric hexagonal boron rings: an inner B_6 ring, a middle B_{12} ring, and an outer B_{18} ring. The structures of B_{35}^- and B_{35} can be viewed as removing a boron atom from the middle B_{12} ring of B_{36}^- and B_{36}, generating an extra hexagonal hole adjacent to the central hexagonal hole such that the two hexagonal holes share a B−B bond to give rise to the DHV. Amazingly, the B−B distances in B_{35}^- and B_{35} exhibit very little change relative to their 36-atom counter parts. In comparison to the symmetric C_{6v} B_{36}, the maximum in-plane dimension in the DHV direction expands by only 0.06 Å in B_{35}^- and shrinks by only 0.09 Å in the perpendicular in-plane direction. The double holes make the

dx.doi.org/10.1021/ja507235s | J. Am. Chem. Soc. 2014, 136, 12257−12260

B_{35}^- cluster slightly more planar with an out-of-plane distortion of 1.12 Å, slightly smaller than that in B_{36} (1.16 Å).[32]

To understand the structure and stability of the 35-atom boron cluster, we analyzed the bonding in the closed-shell B_{35}^- system. All π canonical molecular orbitals (CMOs) of B_{35}^- are plotted in Figure S3 in the SI. Of the 11 CMOs, HOMO-29, HOMO-22, HOMO-26, HOMO-13, and HOMO-15 are the bonding and partial bonding combinations. These CMOs can be transformed to five five-center two-electron (5c-2e) π bonds, as shown in Figure 3a, using the adaptive natural density partitioning

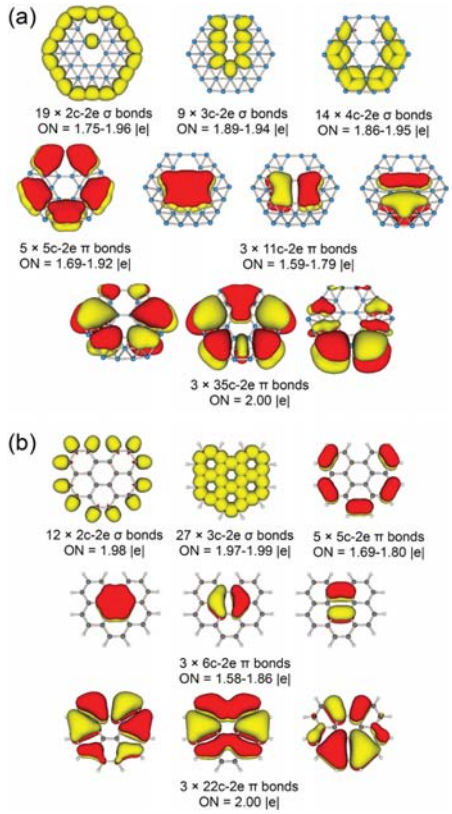

Figure 3. Results of AdNDP analyses for (a) B_{35}^- (C_s, $^1A'$), (b) $C_{22}H_{12}$ (C_{2v}, $^1A_1$). Occupation numbers (ONs) are indicated.

(AdNDP) method.[39] These five bonds mainly describe π interactions between the outer B_{18} ring and the middle B_{11} ring. The remaining six π CMOs can be transformed into two sets of π systems (Figure 3a): three 11c-2e bonds primarily responsible for π bonding between the inner and middle rings, and three 35c-2e global π bonds delocalized over the whole cluster. There are 42 σ CMOs in B_{35}^-. AdNDP analyses (Figure 3a) yielded 19 2c-2e B−B σ bonds involving the 18 peripheral atoms and the B−B bond shared by the double-hexagonal holes, nine 3c-2e σ bonds around the DHV, and 14 4c-2e σ bonds. 2c-2e σ bonds are found for all peripheral atoms in planar boron clusters.[16−23] However, it is rare to see a localized 2c-2e σ bond in the interior of planar boron clusters. It was only observed previously in B_{21}^- between a pair of boron atoms shared by two adjacent pentagonal vacancies.[40]

The π bonding in B_{35}^- is quite interesting. The 11 π bonds from the AdNDP analyses can be viewed to form three different π systems: the five 5c-2e bonds, three 11c-2e bonds, and three 35c-2e bonds, each obeying the $(4n + 2)$ Hückel rule for aromaticity. Thus, the B_{35}^- cluster can be considered to be a unique triply π aromatic system. More interestingly, we found that the π bonding in B_{35}^- is nearly identical to that in the polycyclic aromatic hydrocarbon, benzo(g,h,i)perylene ($C_{22}H_{12}$), as shown in Figure 3b. AdNDP analyses reveal that the 11 π bonds in $C_{22}H_{12}$ can also be classified into three separate π systems, just like that in B_{35}^-. Specifically, the five peripheral C−C 2c-2e π bonds in $C_{22}H_{12}$ are localized, and they correspond to the five 5c-2e π bonds in B_{35}^-. This observation is reminiscent of previous findings that a B_4 or B_5 unit in boron nanoribbons, called polyboroenes, is equivalent to a C−C unit in polyacetylenes.[41−44] The B_{35}^- cluster provides another example of the hydrocarbon analogs of boron clusters: the π bonding in many planar boron clusters has been found to resemble those of aromatic hydrocarbons.[16−23,26−28]

The central hexagonal hole in the C_{6v} B_{36} is critical for its 2D structure. The slight out-of-plane distortion is really due to the peripheral effect, i.e., the peripheral B−B bonds tend to be stronger or slightly shorter than the interior B−B bonds.[32] It is interesting to note that the second hexagonal hole in B_{35}^- or B_{35} induces very little structural distortion and in fact makes the cluster to be slightly more planar, reinforcing the importance of hexagonal vacancies in the stabilization of borophene. The B_{36} cluster has been considered as a motif for borophene consisting of isolated hexagonal holes or the α-sheet. The β-sheet refers to boron monolayers with DHVs or adjacent hexagonal holes.[5] Since the initial predictions of stable α- and β-sheets, many monolayer boron sheets with different hexagonal hole densities and arrangements have been considered.[8−13] We find that the planar B_{35} cluster is in fact a more flexible motif to construct borophenes with DHVs or mixed hexagonal holes and DHVs. Figure 4 shows schematically two such arrangements. Other arrangements of the B_{35} clusters are possible, allowing the creation of borophenes with different hole densities.

In conclusion, we report the structures and bonding of the B_{35}^- and B_{35} clusters, which are found to be quasi-planar structures with a double-hexagonal vacancy or DHV. The structures of B_{35} can be viewed as removing an interior boron

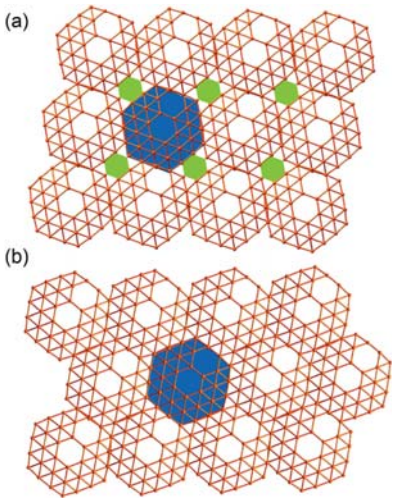

Figure 4. Schematic drawings of borophenes constructed from two different arrangements of the planar hexagonal B_{35} motif. The blue shaded areas represent a single B_{35} unit and the green shaded areas in (a) indicate monohexagonal vacancies as a result of the arrangement of the B_{35} units.

dx.doi.org/10.1021/ja507235s | J. Am. Chem. Soc. 2014, 136, 12257−12260

atom from the hexagonal B_{36} cluster. Chemical bonding analyses show that the closed-shell B_{35}^- cluster possesses three distinct π systems and can be considered to be triply aromatic. The π bonding in B_{35}^- is shown to be analogous to the polycyclic aromatic hydrocarbon, benzo(g,h,i) perylene ($C_{22}H_{12}$). The B_{35} cluster with the DHV is shown to be a new and flexible structural motif, which can be used to construct borophenes related to the β-sheet with DHVs or mixed hexagonal holes and DHVs. The unique structure of B_{35} and its relationship to the β-sheet provide further evidence for the viability of borophene.

■ ASSOCIATED CONTENT

Supporting Information

Methods section. Experimental and computational VDEs, alternative optimized structures at PBE0 level, canonical molecular orbitals, and detailed geometries of B_{35}^-/B_{35}. This material is available free of charge via the Internet at http://pubs.acs.org/.

■ AUTHOR INFORMATION

Corresponding Authors

junli@tsinghua.edu.cn
hj.zhai@sxu.edu.cn
lisidian@sxu.edu.cn
lai-sheng_wang@brown.edu

Notes

The authors declare no competing financial interest.

■ ACKNOWLEDGMENTS

This work was supported by the U.S. National Science Foundation (CHE-1263745), the National Natural Science Foundation of China (21243004, 21373130), and the National Key Basic Research Special Foundations (2011CB932401). H.J.Z. gratefully acknowledges the start-up fund from Shanxi University for support. Part of the calculations was performed using supercomputers at Tsinghua National Laboratory for Information Science and Technology.

■ REFERENCES

(1) Boustani, I.; Quandt, A.; Hernandez, E.; Rubio, A. *J. Chem. Phys.* **1999**, *110*, 3176.
(2) Evans, M. H.; Joannopoulos, J. D.; Pantelides, S. T. *Phys. Rev. B* **2005**, *72*, 045434.
(3) Kunstmann, J.; Quandt, A. *Phys. Rev. B* **2006**, *74*, 035413.
(4) Lau, K. C.; Pandey, R. *J. Phys. Chem. C* **2007**, *111*, 2906.
(5) (a) Tang, H.; Ismail-Beigi, S. *Phys. Rev. Lett.* **2007**, *99*, 115501. (b) Tang, H.; Ismail-Beigi, S. *Phys. Rev. B* **2010**, *82*, 115412.
(6) (a) Yang, X. B.; Ding, Y.; Ni, J. *Phys. Rev. B* **2008**, *77*, 041402. (b) Ding, Y.; Yang, X.; Ni, J. *Appl. Phys. Lett.* **2008**, *93*, 043107.
(7) Galeev, T. R.; Chen, Q.; Guo, J. C.; Bai, H.; Miao, C. Q.; Lu, H. G.; Sergeeva, A. P.; Li, S. D.; Boldyrev, A. I. *Phys. Chem. Chem. Phys.* **2011**, *13*, 11575.
(8) (a) Lau, K. C.; Pandy, R. *J. Phys. Chem. B* **2008**, *112*, 10217. (b) Özdoğan, C.; Mukhopadhyay, S.; Hayami, W.; Güvenç, Z. B.; Pandey, R.; Boustani, I. *J. Phys. Chem. C* **2010**, *114*, 4362.
(9) Penev, E. S.; Bhowmick, S.; Sadrzadeh, A.; Yakobson, B. I. *Nano Lett.* **2012**, *12*, 2441.
(10) Wu, X. J.; Dai, J.; Zhao, Y.; Zhuo, Z. W.; Yang, J. L.; Zeng, X. C. *ACS Nano* **2012**, *6*, 7443.
(11) Yu, X.; Li, L.; Xu, X. X.; Tang, C. C. *J. Phys. Chem. C* **2012**, *116*, 20075.
(12) Lu, H.; Mu, Y.; Bai, H.; Chen, Q.; Li, S. D. *J. Chem. Phys.* **2013**, *138*, 024701.
(13) Banerjee, S.; Periyasamy, G.; Pati, S. K. *J. Mater. Chem. A* **2014**, *2*, 3856.
(14) Liu, Y.; Penev, E. S.; Yakobson, B. I. *Angew. Chem., Int. Ed.* **2013**, *52*, 3156.
(15) Liu, H.; Gao, J.; Zhao, J. *Sci. Rep.* **2013**, *3*, 3238 DOI: 10.1038/srep03238.
(16) (a) Zhai, H. J.; Alexandrova, A. N.; Birch, K. A.; Boldyrev, A. I.; Wang, L. S. *Angew. Chem., Int. Ed.* **2003**, *42*, 6004. (b) Pan, L. L.; Li, J.; Wang, L. S. *J. Chem. Phys.* **2008**, *129*, 024302.
(17) Zhai, H. J.; Kiran, B.; Li, J.; Wang, L. S. *Nat. Mater.* **2003**, *2*, 827.
(18) Kiran, B.; Bulusu, S.; Zhai, H. J.; Yoo, S.; Zeng, X. C.; Wang, L. S. *Proc. Natl. Acad. Sci. U.S.A.* **2005**, *102*, 961.
(19) Alexandrova, A. N.; Boldyrev, A. I.; Zhai, H. J.; Wang, L. S. *Coord. Chem. Rev.* **2006**, *250*, 2811.
(20) Sergeeva, A. P.; Zubarev, D. Y.; Zhai, H. J.; Boldyrev, A. I.; Wang, L. S. *J. Am. Chem. Soc.* **2008**, *130*, 7244.
(21) Huang, W.; Sergeeva, A. P.; Zhai, H. J.; Averkiev, B. B.; Wang, L. S.; Boldyrev, A. I. *Nat. Chem.* **2010**, *2*, 202.
(22) Sergeeva, A. P.; Piazza, Z. A.; Romanescu, C.; Li, W. L.; Boldyrev, A. I.; Wang, L. S. *J. Am. Chem. Soc.* **2012**, *134*, 18065.
(23) (a) Sergeeva, A. P.; Popov, I. A.; Piazza, Z. A.; Li, W. L.; Romanescu, C.; Wang, L. S.; Boldyrev, A. I. *Acc. Chem. Res.* **2014**, *47*, 1349. (b) Popov, I. A.; Piazza, Z. A.; Li, W. L.; Wang, L. S.; Boldyrev, A. I. *J. Chem. Phys.* **2013**, *139*, 144307. (c) Piazza, Z. A.; Popov, I. A.; Li, W. L.; Pal, R.; Zeng, X. C.; Boldyrev, A. I.; Wang, L. S. *J. Chem. Phys.* **2014**, *141*, 034303.
(24) Oger, E.; Crawford, N. R. M.; Kelting, R.; Weis, P.; Kappes, M. M.; Ahlrichs, R. *Angew. Chem., Int. Ed.* **2007**, *46*, 8503.
(25) Romanescu, C.; Harding, D. J.; Fielicke, A.; Wang, L. S. *J. Chem. Phys.* **2012**, *137*, 014317.
(26) Fowler, J. E.; Ugalde, J. M. *J. Phys. Chem. A* **2000**, *104*, 397.
(27) Aihara, J.; Kanno, H.; Ishida, T. *J. Am. Chem. Soc.* **2005**, *127*, 13324.
(28) Zubarev, D. Y.; Boldyrev, A. I. *J. Comput. Chem.* **2007**, *28*, 251.
(29) Moreno, D.; Pan, S.; Zeonjuk, L. L.; Islas, R.; Osorio, E.; Martinez-Guajardo, G.; Chattaraj, P. K.; Heine, T.; Merino, G. *Chem. Commun.* **2014**, *50*, 8140.
(30) Martinez-Guajardo, G.; Sergeeva, A. P.; Boldyrev, A. I.; Heine, T.; Ugalde, J. M.; Merino, G. *Chem. Commun.* **2011**, *47*, 6242.
(31) Jimenez-Halla, J. O. C.; Islas, R.; Heine, T.; Merino, G. *Angew. Chem., Int. Ed.* **2010**, *49*, 5668.
(32) Piazza, Z. A.; Hu, H. S.; Li, W. L.; Zhao, Y. F.; Li, J.; Wang, L. S. *Nat. Commun.* **2014**, *5*, 3113 DOI: 10.1038/ncomms4113.
(33) Li, W. L.; Zhao, Y. F.; Hu, H. S.; Li, J.; Wang, L. S. *Angew. Chem., Int. Ed.* **2014**, *53*, 5540.
(34) Zhai, H. J.; Zhao, Y. F.; Li, W. L.; Chen, Q.; Bai, H.; Hu, H. S.; Piazza, Z. A.; Tian, W. J.; Lu, H. G.; Wu, Y. B.; Mu, Y. W.; Wei, G. F.; Liu, Z. P.; Li, J.; Li, S. D.; Wang, L. S. *Nat. Chem.* **2014**, *6*, 727.
(35) (a) Goedecker, S. *J. Chem. Phys.* **2004**, *120*, 9911. (b) Goedecker, S.; Hellmann, W.; Lenosky, T. *Phys. Rev. Lett.* **2005**, *95*, 055501.
(36) Adamo, C.; Barone, V. *J. Chem. Phys.* **1999**, *110*, 6158.
(37) Li, J.; Li, X.; Zhai, H. J.; Wang, L. S. *Science* **2003**, *299*, 864.
(38) Zhai, H. J.; Kiran, B.; Dai, B.; Li, J.; Wang, L. S. *J. Am. Chem. Soc.* **2005**, *127*, 12098.
(39) Zubarev, D. Y.; Boldyrev, A. I. *Phys. Chem. Chem. Phys.* **2008**, *10*, 5207.
(40) Piazza, Z. A.; Li, W. L.; Romanescu, C.; Sergeeva, A. P.; Wang, L. S.; Boldyrev, A. I. *J. Chem. Phys.* **2012**, *136*, 104310.
(41) Li, W. L.; Romanescu, C.; Jian, T.; Wang, L. S. *J. Am. Chem. Soc.* **2012**, *134*, 13228.
(42) Li, D. Z.; Chen, Q.; Wu, Y. B.; Lu, H. G.; Li, S. D. *Phys. Chem. Chem. Phys.* **2012**, *14*, 14769.
(43) Zhai, H. J.; Chen, Q.; Bai, H.; Lu, H. G.; Li, W. L.; Li, S. D.; Wang, L. S. *J. Chem. Phys.* **2013**, *139*, 174301.
(44) Bai, H.; Chen, Q.; Miao, C. Q.; Mu, Y. W.; Wu, Y. B.; Lu, H. G.; Zhai, H. J.; Li, S. D. *Phys. Chem. Chem. Phys.* **2013**, *15*, 18872.